

**CHAPTER THREE**  
**AXIAL FLOW COMPRESSORS**

### 3.1 Introduction

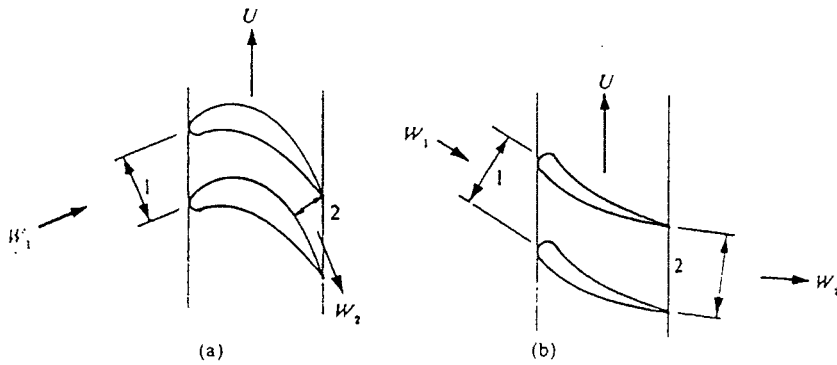


Fig. 3.1 Compressor and turbine blade passage (a) turbine (b) compressor

In studying the flow of the fluid through an axial compressor, it is usual to consider the changes taking place through a compressor stage. A stage consists of a row of moving blades attached to the periphery of a rotor hub followed by a row fixed blades attached to the walls of the outer casing. The compressor is made up of a number of such stages to give an overall pressure ratio from inlet to outlet. Fig 3.2 illustrates a few compressor stages.

It will be seen that at the inlet to the compressor, an extra row fixed vanes, called inlet guide vanes, are fitted. These do not form part of the stage but are solely to guide the air at the correct angle onto the first row of moving blades. The height of the blades is also seen to decrease as the fluid moves through the compressor. This is so that a constant axial velocity through the compressor is maintained as the density increases from the low- to high pressure regions. A constant axial velocity is convenient from the point of view of design but is by no means a requirement. The analysis for flow through the stage will first be described in terms of two-dimensional flow. The flow through the stage is assumed to take place at a mean blade height where the blade peripheral velocities at inlet and outlet are the same, there being no flow in the radial direction. Whirl components of velocity will exist in the direction of blade motion.

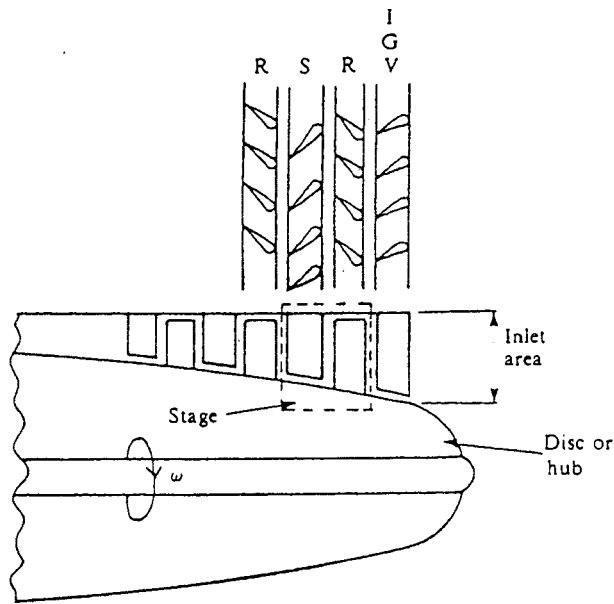


Fig. 3.2 An axial compressor stage

### 3.2 Compressor Stage

The rotor and stator of a stage are shown in Fig 3.3 Note that all angles are referred to the axial velocity vector  $C_a$ .

Air exits from the previous row of stator blades at angle  $\alpha_1$  with absolute velocity  $C_1$ . The rotor row has tangential velocity  $U$ , and combining the two velocity vectors gives the relative inlet velocity vector  $W_1$  at angle  $\beta_1$ . At rotor row outlet the velocity triangles are similar to those drawn for the axial flow pump, and the absolute velocity vector  $C_2$  moves into the stator row where the flow direction is changed to  $\alpha_3$  with absolute velocity  $C_3$ . The diagrams have been drawn showing a large gap between the rotor and stator blades: this is for clarity. In practice, the clearance between rotor and stator rows is small.

If the following stage is the same as the preceding one, the stage is said to be normal. For a normal stage  $C_1 = C_3$  and  $\alpha_1 = \alpha_3$ .  $W_2$  is less than  $W_1$ , showing that diffusion of the relative velocity has taken place with some static pressure rise across the rotor blades. The air is turned towards the axial direction by the blade camber and the effective flow area is increased from inlet to outlet, thus causing diffusion to take place. Similar diffusion of the absolute velocity takes place in the stator, where the absolute velocity vector is again turned towards the axial direction and a further pressure rise occurs.

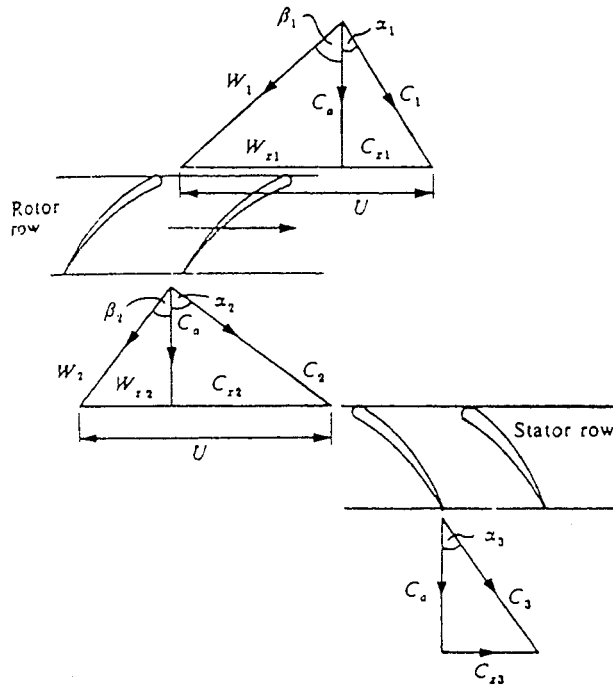


Fig. 3.3 Velocity triangles for an axial flow compressor stage

$$W/m = U_2 C_{x2} - U_1 C_{x1} \quad (3.1)$$

$$\text{or } E = (U_2 C_{x2} - U_1 C_{x1})/g$$

But from the velocity triangles and noting that  $C_a$  is constant through the stage, and  $U_1 = U_2 = U$ ,

$$C_{x2} = U - C_a \tan \beta_2$$

and

$$C_{x1} = U - C_a \tan \beta_1$$

Thus

$$C_{x2} - C_{x1} = C_a (\tan \beta_1 - \tan \beta_2)$$

and

$$E = UC_a (\tan \beta_1 - \tan \beta_2)/g \quad (W/(N/s)) \quad (3.2)$$

The energy transfer may also be written in terms of the absolute velocity flow angles.

Equation (3.2) or (3.3) may be used depending upon the information available.

The flow through the stage is shown thermodynamically on the Mollier chart in Fig 3.4 and is similar to that for a centrifugal compressor. The enthalpy change is continuous taking account of irreversibilities in the rotor and stator.

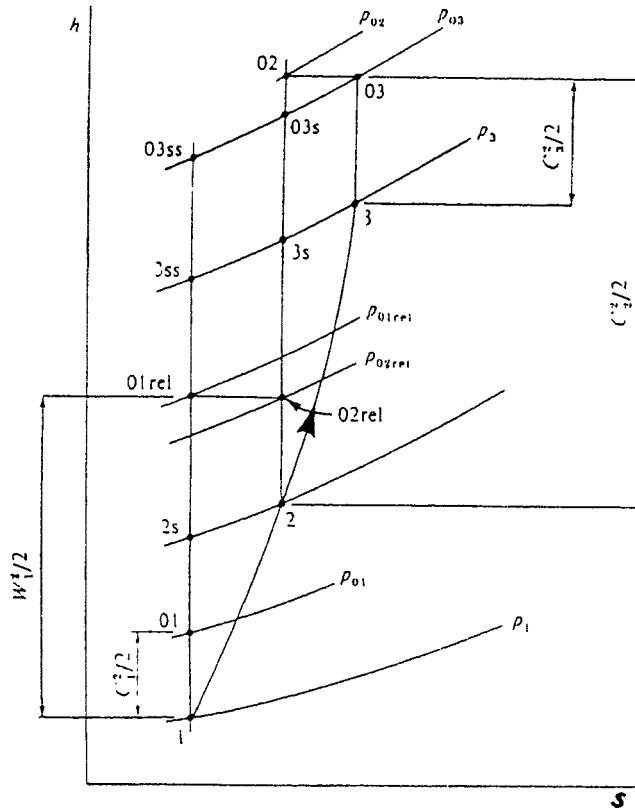


Fig. 3.4 Mollier chart for an axial flow compressor stage

Assuming adiabatic flow through the stage,  $h_{03} = h_{02}$ , and therefore Eq (3.1) may be written as

$$W/m = h_{02} - h_{01} \quad (W \text{ (kg/s)}) \quad (3.4)$$

Writing

$$h_0 = h + C^2/2 = h + (C_a^2 + C_x^2)/2$$

$$(h_2 - h_1) - (C_{x2} - C_{x1}) [2U - (C_{x2} + C_{x1})]/2 = 0$$

Rearranging

$$(h_2 - h_1) - (C_{x2} - C_{x1}) [(U - C_{x2}) + (U - C_{x1})]/2 = 0$$

$$(h_2 - h_1) + (W_{x2} - W_{x1}) (W_{x2} + W_{x1})/2 = 0$$

$$(h_2 - h_1) + (W_{x2}^2 - W_{x1}^2)/2 = 0$$

But  $(W_{x2}^2 - W_{x1}^2) = (W_2^2 - W_1^2)$  since  $C_a$  is constant. therefore

$$h_2 + W_2^2/2 = h_1 + W_1^2/2 \quad (3.5)$$

and eq (3.5) can be written

$$h_{02rel} = h_{01rel} \quad (3.6)$$

Where the relative total enthalpy is based on the relative velocity.

equation (3.6) shows that the total enthalpy based on relative velocities in the rotor is constant across the rotor and this result is also valid for the axial flow gas turbine rotor. The relative velocity may be of the same order of magnitude, but the axial flow compressor receives no contribution from the change in tangential velocity.

The isentropic efficiency is written as

$$\eta_c = \frac{\text{Ideal isentropic work input}}{\text{Actual work input}}$$

$$= \frac{(h_{03ss} - h_{01})}{(h_{03} - h_{01})}$$

which reduces to

$$\eta_c = T_{01} (T_{03ss}/T_{01} - 1) / (T_{03} - T_{01})$$

Putting

$$P_{03}/P_{01} = (T_{03ss}/T_{01})^{\gamma/(\gamma-1)}$$

the pressure ratio becomes

$$P_{03}/P_{01} = [1 + \eta_c (T_{03} - T_{01}) / T_{01}]^{\gamma/(\gamma-1)} \quad (3.7)$$

The energy input to the fluid will be absorbed usefully in raising the pressure and velocity of the air and some will be wasted in overcoming various frictional losses. However the whole of the work input will appear as a stagnation temperature rise of the air regardless of the isentropic efficiency.

In practice  $C_a$  is not constant along the length of the blade to account for this, a work done factor  $\lambda$  is introduced, defined as

$$\text{Work done factor} = \frac{\text{Actual work absorbing capacity}}{\text{Ideal work absorbing capacity}}$$

Hence

$$(T_{03} - T_{01}) = \lambda UC_a (\tan \beta_1 - \tan \beta_2) / C_p \quad (3.9)$$

Figure 3.5 illustrates that it is only inlet of the machine that the velocity profile is fairly constant over the blade length. the solid boundaries of the rotor and stator exert more and more influence on the velocity profile as the air moves through the compressor. The variation in work done factor in Fig 3.6 shows  $\lambda$  decreases as the number of compressor stages increases.

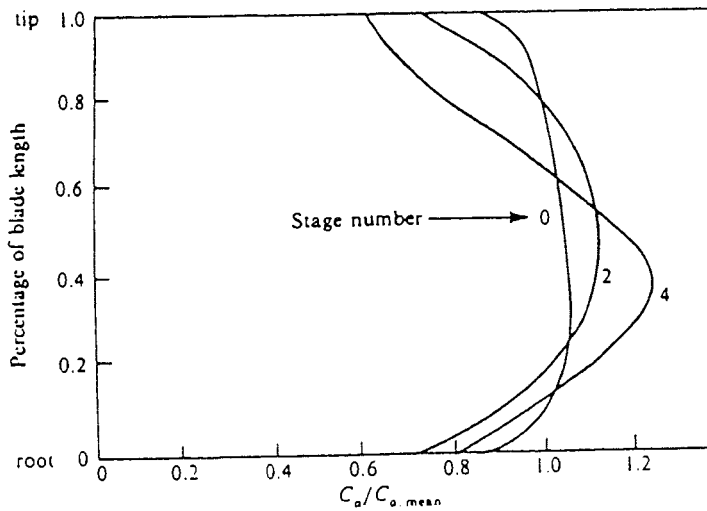


Fig. 3.5 Variation of axial velocity along a blade

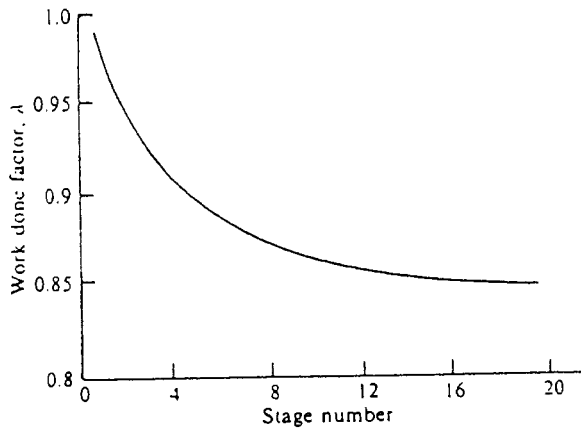


Fig. 3.6 Variation of work done factor with number of stages

### 3.3 Reaction Ratio

The reaction ratio is a measure of the static enthalpy rise that occurs in the rotor expressed as a percentage of the total static enthalpy rise across the stage. It is defined as

$$R = \frac{\text{Static enthalpy rise in rotor}}{\text{Static enthalpy rise in stage}}$$

$$= (h_2 - h_1) / (h_3 - h_1) \tag{3.10}$$

Since  $h_{01rel} = h_{02rel}$  then

$$(h_2 - h_1) = (W_1^2 - W_2^2)/2$$

Also if  $C_1 = C_3$  then

$$(h_3 - h_1) = (h_{03} - h_{01}) = U (C_{x2} - C_{x1})$$

and substituting for  $(h_2 - h_1)$  and  $(h_3 - h_1)$  in Eq (3.10) the reaction ratio becomes

$$\begin{aligned} R &= (W_1^2 - W_2^2) / [2U (C_{x2} - C_{x1})] \\ &= [(C_a^2 + W_{x1}^2) - (C_a^2 + W_{x2}^2)] / [2U (C_{x2} - C_{x1})] \\ &= (W_{x1} + W_{x2}) (W_{x1} - W_{x2}) / [2U (C_{x2} - C_{x1})] \end{aligned}$$

But  $C_{x2} = U - W_{x2}$  and  $C_{x1} = U - W_{x1}$ . Therefore

$$(C_{x2} - C_{x1}) = (W_{x1} - W_{x2})$$

Hence

$$\begin{aligned} R &= (W_{x1} + W_{x2}) / 2U \\ &= C_a (\tan \beta_1 + \tan \beta_2) / 2U \\ &= (C_a / U) (\tan \beta_\alpha) \\ &= \phi \tan \beta_\alpha \end{aligned} \tag{3.11}$$

Here  $\tan \beta_\alpha = (\tan \beta_1 + \tan \beta_2) / 2$ . while the ratio of axial velocity to blade speed is called the flow coefficient.

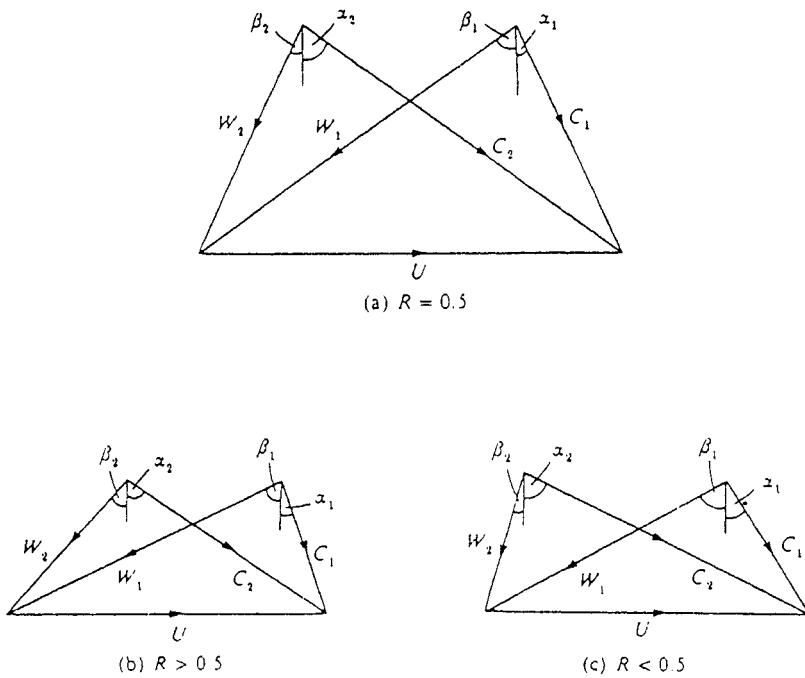


Fig. 3.7 Effect of reaction ratio on the velocity triangles

For a reaction ratio of 50 per cent.  $(h_2 - h_1) = (h_3 - h_2)$ , that is the static enthalpy and temperature increase in the rotor and stator are equal. Also from Eq (3.12)  $\beta_2 = \alpha_1$  and when the outlet and inlet velocity triangles are superimposed, the resulting diagram is symmetrical. This is shown in fig 3.7a. For  $R > 0.5$ . Fig 3.7b shows the diagram skewed to the right since  $\beta_2 > \alpha_1$  and the static enthalpy rise in the rotor is greater than in the stator. The static pressure rise is also greater in the rotor than the stator. If

$R < 0.5$  the diagram is skewed to the left as in fig 5.7c, and static enthalpy and pressure rises are greater in the stator than in the rotor. A reaction ratio of 50 percent is usually chosen so that the adverse pressure gradient over the stage is shared equally by the stator and rotor. This decreases the likelihood of boundary-layer separation in both the stator and rotor blades and is the condition for maximum temperature rise and efficiency.

### 3.4 Stage Loading

If the power input is divided by the term  $mU^2$ , a dimensionless coefficient  $\psi$

$$\psi = W/mU^2 = (h_{03} - h_{01})/U^2 \quad (3.13)$$

$$= \lambda (C_{x2} - C_{x1})/U$$

$$= \lambda (C_a/U) (\tan \alpha_2 - \tan \alpha_1)$$

$$\psi = \lambda \phi (\tan \alpha_2 - \tan \alpha_1) \quad (3.14)$$

### 3.5 Lift And Drag coefficients

Consider the rotor shown in Fig 3.8 with relative velocity vectors  $W_1$  and  $W_2$  at angles  $\beta_1$  and  $\beta_2$ . This system is similar to flow over an aerofoil so that lift and drag forces will be set up on the blade while the forces on the air will act in the opposite direction as shown in Fig 3.9.

The drag force is defined as acting in the line of the mean velocity vector  $W_\alpha$  at angle  $\beta_\alpha$  to the axial direction as defined by Eq (3.11), and the lift force acts perpendicular to this.

The resultant force experienced by the air is therefore given by the vector R in Fig 3.9. so that the force acting in the direction of blade rotation (the x direction) is written as

$$\begin{aligned} F_x &= L \cos \beta_\alpha + D \sin \beta_\alpha \\ &= L \cos \beta_\alpha [ 1 + (C_D/C_L) \tan \beta_\alpha ] \end{aligned}$$

But the lift coefficient is defined as

$$C_L = L / 0.5 \rho W_\alpha^2 A$$

Where the blade area is the product of the chord  $c$  and the span  $l$ , and putting

$W_\alpha = C_a / \cos \beta_\alpha$  then

$$F_x = \rho C_a^2 c l C_L \sec \beta_\alpha [ 1 + (C_D/C_L) \tan \beta_\alpha ] / 2$$

The power delivered to the air is given by

$$\begin{aligned} U F_x &= m (h_{03} - h_{01}) (W) \\ &= \rho C_a l s (h_{03} - h_{01}) \end{aligned}$$

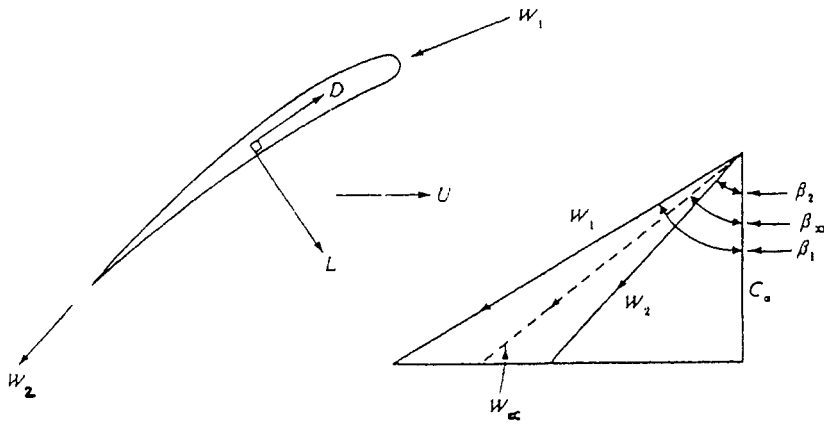


Fig. 3.8 Velocity triangle of rotor blade

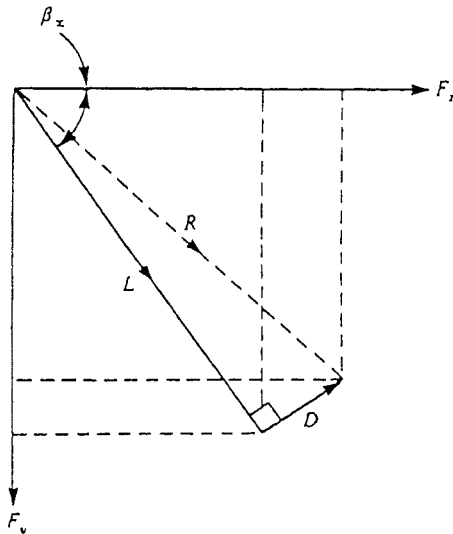


Fig. 3.9 Resolving blade forces into the direction of rotation.

Where the flow through one blade passage of width  $s$  has been considered.

Therefore

$$\begin{aligned}
 \psi &= (h_{03} - h_{01}) / U^2 \\
 &= F_x / \rho C_a s U \\
 &= (C_a / U) (c/s) \sec \beta_\alpha (C_L + C_D \tan \beta_\alpha) / 2 \\
 &= \phi (c/s) \sec \beta_\alpha (C_L + C_D \tan \beta_\alpha) / 2
 \end{aligned} \tag{3.15}$$

For maximum efficiency, the mean flow angle  $\beta_\alpha$  is usually about  $45^\circ$  and substituting for this into Eq. (3.15) the optimum blade loading factor  $\psi_{opt}$  becomes

$$\psi_{opt} = (\phi/\sqrt{2}) (c/s) (C_L + C_D) \tag{3.16}$$

If  $C_D$  is much smaller than  $C_L$ , which is usually the case for a well -designed blade. then.

### 3.6 Blade Cascades

A cascade is a row of geometrically similar blades arranged at equal distances from each other and aligned to the flow direction as shown in Fig 3.10 . The row of blades is installed on a turntable at the end of a wind tunnel channel such that the angle of incidence of the blades with respect to the

approaching air may be varied. Vertical traverses between successive blades may than be made with pitot tubes, and yaw meters to determine pressure losses and air flow angles. Figure 3.10 is known as a linear cascade and can be imagined as a row of compressor blades unwound from the rotor to form the cascade. The number of blades comprising the cascade has to be sufficient to eliminate any wind tunnel wall boundary-layer effects, and suction slots are often let into the tunnel walls to control the boundary layer.



The data obtained from cascade testing have to be corrected before application to a prototype compressor can be made. The reasons for the corrections are because of the differences between flow in the actual machine and flow through the cascade. These differences are as follows:

1. In the machine, annulus wall boundary layers exist at the blade hub and tip.
2. In the machine, alternate blade rows interfere with the perceived cascade data flow pattern.
3. In the machine, the solidity decreases from hub to tip.
4. Blade velocity varies from hub to tip, thereby affecting the blade inlet angle.

From 3 and 4 it is evident that a cascade test only applies for one radius and inlet angle, and therefore it may be necessary to carry out a number of tests to obtain a reliable picture of the flow in the blades.

### 3.6.1 Cascade Nomenclature and Curves

Before venturing further into cascade testing and blade design, it is necessary to define various important angles relevant to the design. In Fig 3.11 a cambered blade is shown with a curved camber line through the centre.

The tangents to the camber line at inlet and outlet are the camber angles  $\alpha'_1$  and  $\alpha'_2$  to the axial direction respectively. The blade camber angle  $\theta$  is defined as  $(\alpha'_1 - \alpha'_2)$ . The chord  $c$  is the distance

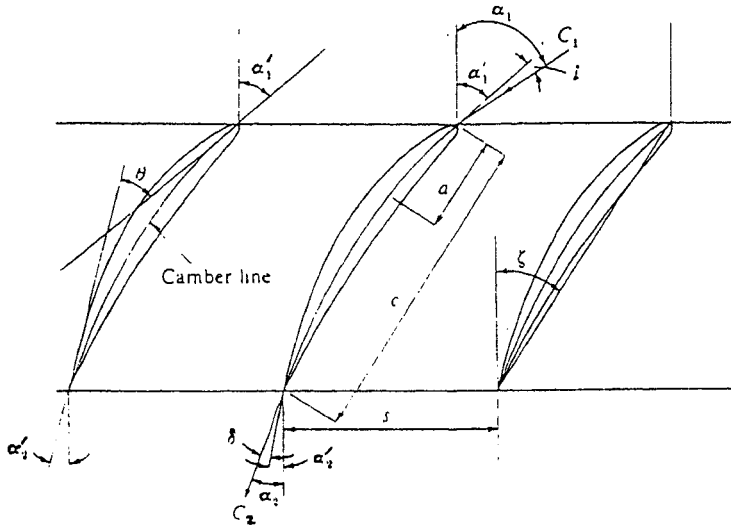


Fig. 3.11 Cascade nomenclature

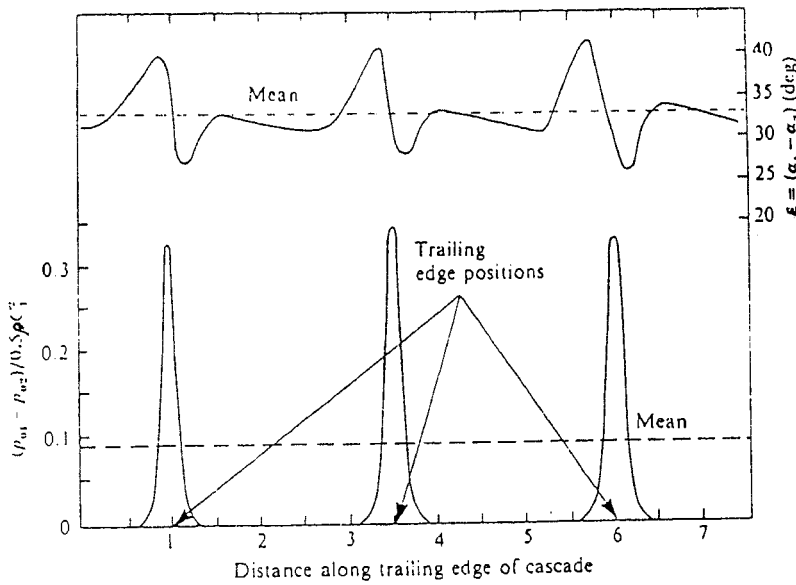


Fig. 3.12 Cascade deflection and pressure loss curves at one angle of incidence.

blade inlet and trailing edges. The stagger angle  $\xi$  is that between the axial direction and the chord and represents the angle at which the blade is set in the cascade. The blade spacing is  $s$  and represents the blade pitch. If the air enters with velocity  $C_1$  at angle  $\alpha_1$ , the angle of incidence  $i$  is  $(\alpha_1 - \alpha'_1)$ . The air leaves the blade with velocity  $C_2$  at angle  $\alpha_2$  and the difference  $(\alpha_2 - \alpha'_2)$  is the deviation angle  $\delta$ . The air deflection angle is  $\epsilon (= \alpha_1 - \alpha_2)$  and it is this angle along with the cascade inlet and outlet stagnation pressure  $p_{01}$  and  $p_{02}$  that are measured in the traverse along  $s$ . The results of the traverses are usually presented as in Fig 3.12, the stagnation pressure loss being plotted as a dimensionless number given by

$$\text{Stagnation pressure loss coefficient} = (P_{01} - P_{02}) / 0.5 \rho C_1^2 \quad (3.18)$$

A number of curves such as Fig. 3.12 are obtained for different incidence angles and the mean deflection and pressure loss coefficient for each curve,  $\bar{\epsilon}$  and  $(\overline{P_{01} - P_{02}}) / 0.5 \rho C_1^2$ , are plotted against incidence angle as in Fig 3.13. The deflection increases with angle of incidence up to a maximum  $\epsilon_s$ . This is the stall point where separation occurs on the suction surface of the blade, and since this angle may not be well defined in some designs, it is taken as the angle of incidence where the mean pressure loss is twice the minimum. It is evident that for a wide range of incidence the pressure loss is fairly constant and it is possible to select an angle of deflection  $\epsilon^*$  that is also compatible with low pressure loss as representative for the particular design and by convention  $\epsilon^* = 0.8 \epsilon_s$ . The normal

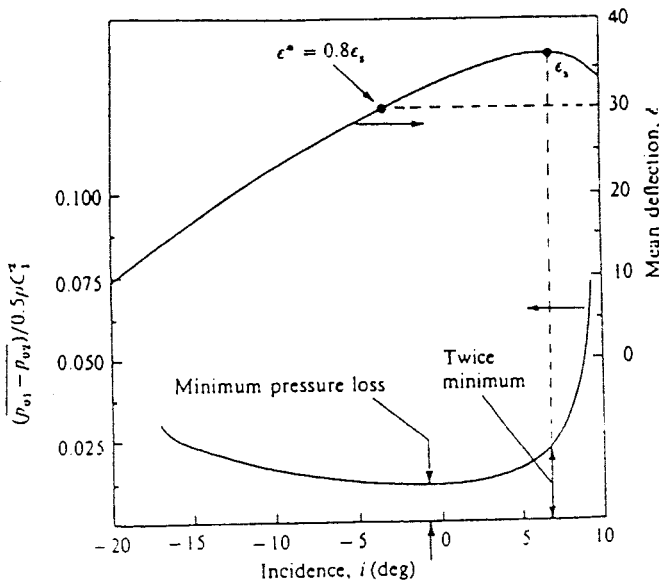


Fig. 3.13 Cascade mean deflection and pressure loss curves.

deflection angle  $\epsilon^*$  is dependent mainly on the pitch/chord ratio ( $s/c$ ) and  $\alpha_2$ , this being determined from a large number of cascade tests. It is thus possible to plot a set of master curves of  $\epsilon^*$  versus  $\alpha_2$  for different values of ( $s/c$ ). These curves are particularly useful to the designer when any two of the three variables are fixed. For example if the rotor inlet and outlet angle  $\beta_1$  and  $\beta_2$  are known,  $\epsilon^*$  can be found and at angle  $\beta_2$  ( $s/c$ ) can be read from Fig 3.14.

The deviation angle  $\delta$  is caused by the air not remaining attached to the blade over its total curvature  $\delta$  is given by the empirical relationship

$$\delta = m\theta (s/c)^{1/2} \quad (3.19)$$

Where

$$m = 0.23 (2a/c)^2 + 0.1 (\alpha_2/50) \quad (3.20)$$

and  $a$  is the distance long the chord to the point of maximum camber. For a circular arc camber line,  $(2a/c) = 1$  and this blade form is often chosen.

### 3.6.2 Cascade Lift and Drag Coefficients

The pressure ratio is governed by the efficiency of the stage and this efficiency depends on the total drag for both the rotor and stator rows. From the measured cascade test result of  $(p_{01} - p_{02})$  the lift coefficient  $C_L$  and drag coefficient  $C_D$  may be obtained, where  $C_D$  is the blade profile drag. The method of approach is to equate all forces acting on the air to the rate of change of momentum of the air.

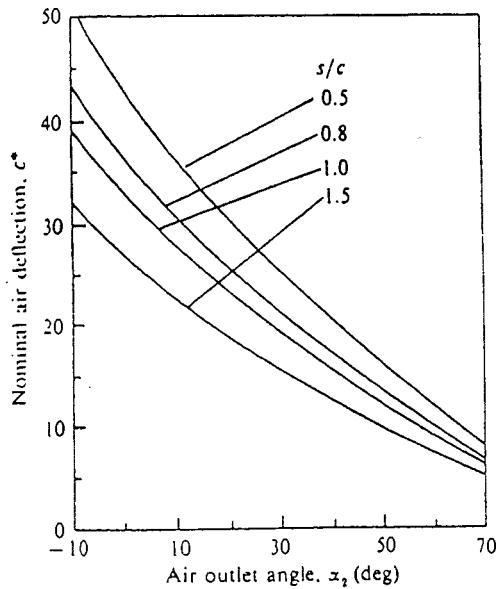


Fig. 3.14 Cascade nominal deflection versus air outlet angle

In Fig 3.15 two blades of a cascade having chord  $c$  and pitch  $s$  are shown. At sections 1 and 2 the total air pressure are  $p_{01}$  and  $p_{02}$  respectively with corresponding velocities of  $C_1$  and  $C_2$ , while the density change across the cascade is negligible. The static pressure change across cascade is therefore given by

$$(p_2 - p_1) = \rho(C_1^2 - C_2^2)/2 - \overline{(P_{01} - P_{02})} \quad (3.21)$$

Where it should be noted that  $p_{01} > p_{02}$  because no work is done in the cascade and the flow is irreversible. Equation (3.21) will be written as

$$\Delta p = \rho(C_1^2 - C_2^2)/2 - \overline{P_0} \quad (3.22)$$

Where  $\Delta p = (p_2 - p_1)$  and  $\overline{P_0} = \overline{(P_{01} - P_{02})}$

The summation of all forces acting on the air in the control volume in the x and y directions must equal the rate of change of momentum of the air in these directions. Considering first the y direction, since  $C_a$  is constant, there is no velocity change from 1 to 2 in the y direction and consequently no momentum change. Hence for a unit length of blade,

$$L \sin \alpha_\alpha - D \cos \alpha_\alpha - s\Delta p = 0$$

Therefore

$$D = L \tan \alpha_\alpha - s\Delta p / \cos \alpha_\alpha \quad (3.23)$$

In the x direction the velocity changes from  $C_{x1}$  to  $C_{x2}$  and nothing that these are in the negative x direction,

$$\begin{aligned} L \cos \alpha_\alpha + D \sin \alpha_\alpha &= -\rho C_a s (C_{x2} - C_{x1}) \\ &= \rho C_a^2 s (\tan \alpha_1 - \tan \alpha_2) \end{aligned}$$

and rearranging

$$L = (\rho C_a^2 s / \cos \alpha_\alpha) (\tan \alpha_1 - \tan \alpha_2) - D \tan \alpha_\alpha \quad (3.24)$$

Substituting for L and  $\Delta p$  in Eq. (3.23)

$$\begin{aligned} D &= [(\rho C_a^2 s / \cos \alpha_\alpha) (\tan \alpha_1 - \tan \alpha_2) - D \tan \alpha_\alpha] \tan \alpha_\alpha \\ &\quad - (s / \cos \alpha_\alpha) [\rho (C_1^2 - C_2^2) / 2 - \bar{p}_0] \end{aligned}$$

and

$$\begin{aligned} D(1 + \tan^2 \alpha_\alpha) &= (\rho C_a^2 s / \cos \alpha_\alpha) (\tan \alpha_1 - \tan \alpha_2) \tan \alpha_\alpha \\ &\quad - (s / \cos \alpha_\alpha) [\rho (C_1^2 - C_2^2) / 2 - \bar{p}_0] \end{aligned}$$

Now  $(1 + \tan^2 \alpha_\alpha) = \sec^2 \alpha_\alpha$  and  $\tan \alpha_\alpha = (\tan \alpha_1 + \tan \alpha_2) / 2$ . Therefore

$$\begin{aligned} D / \cos^2 \alpha_\alpha &= (\rho C_a^2 s / 2 \cos \alpha_\alpha) (\tan \alpha_1 - \tan \alpha_2) (\tan \alpha_1 + \tan \alpha_2) \\ &\quad - (s / \cos \alpha_\alpha) [\rho (C_1^2 - C_2^2) / 2 - \bar{p}_0] \end{aligned}$$

and noting that

$$[C_1^2 - C_2^2] = C_a^2 (\tan^2 \alpha_1 - \tan^2 \alpha_2)$$

then

$$\begin{aligned} D / \cos^2 \alpha_\alpha &= (\rho C_a^2 s / 2 \cos \alpha_\alpha) (\tan^2 \alpha_1 - \tan^2 \alpha_2) \\ &\quad - (\rho C_a^2 s / 2 \cos \alpha_\alpha) (\tan^2 \alpha_1 - \tan^2 \alpha_2) \\ &\quad + (\bar{s} \bar{p}_0 / \cos \alpha_\alpha) \end{aligned}$$

The first two terms on the RHS are equal and therefore disappear to leave

$$D = \bar{s} \bar{p}_0 \cos \alpha_\alpha$$

Dividing the drag by  $0.5 \rho C_\alpha^2 c$  gives the drag coefficient

$$C_D = 2(s/c) (\bar{p}_0 / \rho C_x^2) \cos \alpha_\alpha \quad (3.25)$$

But  $C_{\alpha} = C_a / \cos \alpha_{\alpha}$  and  $C_a = C_1 \cos \alpha_1$  thus substituting in Eq (3.25) gives

$$C_D = 2(s/c) (\bar{p}_0 / \rho C_1^2) (\cos^3 \alpha_{\alpha} / \cos^2 \alpha_1) \quad (3.26)$$

A similar procedure may be followed for  $C_l$  by substituting for  $D$  and  $\Delta p$  in Eq (3.24) to give

$$L = (\rho C_a^2 s / \cos \alpha_{\alpha}) (\tan \alpha_1 - \tan \alpha_2) - \{L \tan \alpha_{\alpha} - (s / \cos \alpha_{\alpha}) [\rho(C_1^2 - C_2^2) / 2 - \bar{p}_0]\} \tan \alpha_{\alpha} \text{ and}$$

$$L (1 + \tan^2 \alpha_{\alpha}) = (\rho C_a^2 s / \cos \alpha_{\alpha}) (\tan \alpha_1 - \tan \alpha_2) + (s \rho C_a^2 / 2 \cos \alpha_{\alpha}) (\tan^2 \alpha_1 - \tan^2 \alpha_2) \tan \alpha_{\alpha} - (\bar{s} \bar{p}_0 / \cos \alpha_{\alpha}) \tan \alpha_{\alpha}$$

$$\begin{aligned} L &= (\rho C_a^2 s \cos \alpha_{\alpha}) [(\tan \alpha_1 - \tan \alpha_2) + (\tan^2 \alpha_1 - \tan^2 \alpha_2) (\tan \alpha_1 + \tan \alpha_2) / 4] - (\bar{s} \bar{p}_0 \cos \alpha_{\alpha}) \tan \alpha_{\alpha} \\ &= (\rho C_a^2 s \cos \alpha_{\alpha}) (\tan \alpha_1 - \tan \alpha_2) [1 + (\tan \alpha_1 + \tan \alpha_2)^2 / 4] - (\bar{s} \bar{p}_0 \cos \alpha_{\alpha}) \tan \alpha_{\alpha} \\ &= (\rho C_a^2 s \cos \alpha_{\alpha}) (\tan \alpha_1 - \tan \alpha_2) / \cos^2 \alpha_{\alpha} - (\bar{s} \bar{p}_0 \cos \alpha_{\alpha}) \tan \alpha_{\alpha} \text{ Now} \end{aligned}$$

$$C_L = L / 0.5 \rho C_x^2 c = 2L \cos^2 \alpha_{\alpha} / \rho C_a^2 c = 2L \cos^2 \alpha_{\alpha} / \rho C_1^2 c \cos^2 \alpha_1 \text{ Thus}$$

$$\begin{aligned} C_L &= 2(s/c) \cos \alpha_{\alpha} (\tan \alpha_1 - \tan \alpha_2) - 2(s/c) (\bar{p}_0 / \rho C_1^2) (\cos^3 \alpha_{\alpha} / \cos^2 \alpha_1) \tan \alpha_{\alpha} \\ &= 2(s/c) \cos \alpha_{\alpha} (\tan \alpha_1 - \tan \alpha_2) - C_D \tan \alpha_{\alpha} \end{aligned} \quad (3.27)$$

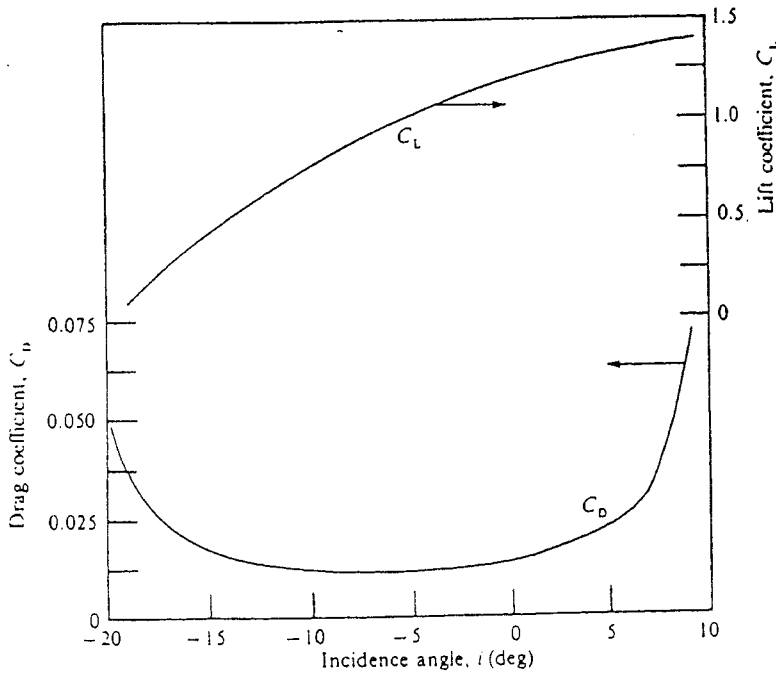


Fig. 3.16 Lift and drag coefficients for the cascade from Eqs. (3.26) and (3.27)

The air inlet velocity  $C_1$ , the incidence angle  $i$  and the blade inlet angle  $\alpha'_1$  are known and therefore  $\alpha_1 (= \alpha'_1 + i)$  is also known. The deviation  $\epsilon$  is read from Fig 3.13 for the angle of incidence, and  $\alpha_\alpha = \tan^{-1} [(\tan \alpha_1 + \tan \alpha_2)/2]$  where  $\alpha_2 = (\alpha_1 - \epsilon)$

Knowing  $(s/c)$ , values of  $\sqrt{p_0}/0.5 \rho C_1^2$  can be read from Fig 3.13 for various incidence angles and upon substitution of these variables into Eqs (3.26) and (3.27) curves of  $C_L$  and  $C_D$  may be plotted against the incidence angle as shown in Fig 3.16. Finally the lift coefficient can be plotted against the air outlet angle  $\alpha_2$  for the normal value of  $\epsilon^*$  for a whole series of different geometry cascades to give the variation of  $C_L$  with air outlet angle for a particular  $(s/c)$  ratio (Fig 3.17).

The drag coefficient is usually very small in comparison with  $C_L$  and is therefore often ignored so that Eq. (3.27) becomes.

$$C_L = 2(s/c) \cos \alpha_\alpha (\tan \alpha_1 - \tan \alpha_2) \quad (3.28)$$

To the profile drag as given by Eq. (3.26) two further drags must be added. These are the drag effects due to the walls of the compressor, usually called the annulus drag and the secondary losses caused by trailing vortices at the blade tips. Empirical relationships exist for these drags as follows.

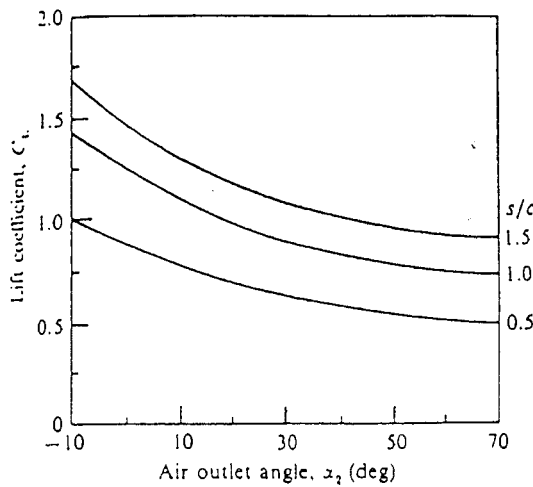


Fig. 3.17 Normal lift coefficients for the cascade

Annulus drag coefficient

$$C_{DA} = 0.02 (s/l) \quad (3.29)$$

where  $l$  is the blade height

Secondary losses

$$C_{DS} = 0.018 C_L^2 \quad (3-30)$$

The total drag coefficient is given by

$$C_{DT} = C_D + C_{DA} + C_{DS} \quad (3.31)$$

### 3.7 Blade Efficiency and Stage Efficiency

It has been shown in the previous section that linear cascade data may be effectively used to determine the lift and drag coefficients for the cascade and then be modified by the addition of annulus drag and secondary losses in order to approximate drag coefficient for an annular cascade. After determining  $C_{DT}$  from Eq. (3.31), the pressure loss coefficient  $\bar{p}_o / 0.5 \rho C^2_1$  is determined from Eq. (3.26). The blade row efficiency  $\eta_b$  is defined as.

$$\eta_b = \frac{\text{Actual pressure rise in compressor blade row}}{\text{Theoretical pressure rise in blade row}} \quad (3.32)$$

Now the theoretical pressure rise will occur when  $\bar{p}_o$  is zero, that is when there is no total pressure loss across the cascade. Therefore from Eq. (3.22)

$$\Delta p_{\text{theor}} = \rho C_a^2 (\tan^2 \alpha_1 - \tan^2 \alpha_2) / 2 \quad (3.33)$$

and blade efficiency is defined as

$$\begin{aligned} \eta_b &= (\Delta \bar{p}_{\text{theor}} - p_o) / \Delta p_{\text{theor}} \\ &= 1 - \bar{p}_o / \Delta p_{\text{theor}} \end{aligned} \quad (3.34)$$

Where both actual and theoretical static pressure differences are expressed in terms of known angles.

For the normal stage,  $C_1 = C_3$ , and therefore the stage isentropic efficiency can be approximated to

$$\eta_s = (T_{3ss} - T_1) / (T_3 - T_1) \quad (3.35)$$

It can be shown that for reaction ratios of 50 percent, where  $(T_2 - T_1)$  in the rotor will equal  $(T_3 - T_2)$  in the stator, the blade efficiency and stage isentropic efficiencies are the same. For other reaction ratios, the stage efficiency is given by

$$\eta_s = R \eta_{\text{brotor}} + (1 - R) \eta_{\text{bstator}} \quad (3.36)$$

If, for 50 per cent reaction, total values are used instead of static values, then the total-to-total pressure ratio is approximately equal to the static-to-static pressure ratio.

### 3.8 Three-Dimensional Flow

So far we have been considering only those flows that are two-dimensional in nature in that only whirl and axial flow velocities exist with no radial velocity component. In axial flow turbomachines with hub/tip ratios greater than 0.8 this is a fairly reasonable assumption concerning the flow in the annulus. but for hub /tip ratios less than 0.8, the assumption of two-dimensional flow is no longer valid. This is seen so be to in the case of aircraft compressors, and at the low-pressure end of gas turbines where because of the high mass flow requirements and the need for as small a frontal area as possible

the trend is to longer blades on a smaller hub. Radial velocities set up in the blade row can now result in an appreciable redistribution of the mass flow, which can seriously affect the blade outlet velocity distribution. Consequently any blade designed on the two-dimensional principle could be seriously in error as regards blade angles.

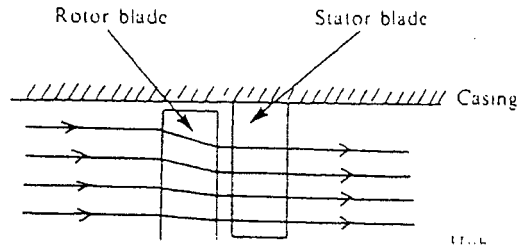


Fig. 3.18 Streamline deviation

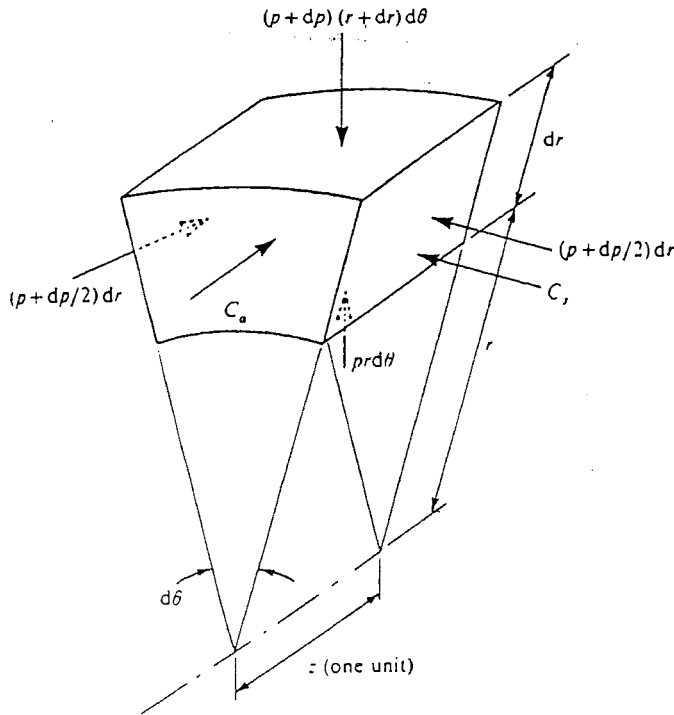


Fig. 3.19 Pressure forces on a fluid element

Radial flow is caused by a temporary imbalance between the centrifugal and radial pressure forces acting on the fluid. When these forces balance each other, there is no radial velocity and the fluid is said to be in radial equilibrium. The method of analysis is known as the 'radial equilibrium method' and assumes that all radial movement of the streamlines takes place in the rotating blade passages, while on

either side the streamlines are two-dimensional as illustrated in Fig 3.18. The analysis examines the pressure forces acting on an element of fluid, shown in Fig 3.19 and equates these forces to the centrifugal forces acting on the fluid. The stagnation enthalpy  $h_0$  at any radius is then introduced and the following equation is derived.

$$dh_0/dr = C_x^2/r + C_x dC_x/dr + C_a dC_a/dr \quad (3.37)$$

Equation (3.37) is the radial equilibrium equation and may be applied to problems in different ways. For instance, if it is assumed that the energy transfer is constant at all radii, then  $dh_0/dr = 0$  and

$$C_x^2/r + C_x dC_x/dr + C_a dC_a/dr = 0 \quad (3.38)$$

$C_a$  is constant over the annulus, then  $dC_a/dr = 0$  and hence

$$dC_x/dr = -C_x/r \quad (3.39)$$

which upon integration gives

$$C_x r = \text{const} \quad (3.40)$$

and this is the requirement for flow in a free vortex with the whirl velocity being inversely proportional to the radius. The outlet blade angles would therefore be calculated using the free vortex velocity distribution.

It is not necessary to stipulate that  $dh_0/dr$  be zero or indeed that  $C_a$  is constant at all radii. It might be desirable to specify a radial distribution of energy transfer, choose a radial distribution for  $C_a$  and calculate  $C_x$  as a function of  $r$  which satisfies Eq. (3.37). Having discussed the principle of three-dimensional analysis, however, it should be stressed that it is not a panacea for all design problems since loss of performance due to boundary-layer growth and secondary losses detract even from the improved accuracy of radial equilibrium analysis.

### 3.9 Multi-Stage Performance

The total pressure ratio across a single stage is dependent upon the total temperature rise across the stage, and the unthinking might assume that, to find the total pressure ratio across  $N$  stages, it would only be necessary to raise the pressure ratio to the power of the number of stages, such that if  $p_{or}$  is the pressure ratio for one stage, then the total pressure ratio is given by  $(p_{or})^N$ . However, this is not correct, since for the same temperature rise per stage, as the entropy increases, the pressure rise decreases, as examination of the Mollier chart will show. It is here that the small stage or polytropic efficiency  $\eta_p$  is employed.

In Fig 3.20, if we compress in a single compression from 1 to 5 the isentropic work done is

$$W/m = (h_{1s} - h_1)$$

and the isentropic efficiency of the compression is

$$\eta_c = (h_{11s} - h_1) / (h_{11} - h_1)$$

If we now compress from 1 to 5 in a number of small finite stages, the isentropic work done is

$$W_s/m = (h_{2s} - h_1) + (h_{3s} - h_2) + (h_{4s} - h_3) + (h_{5s} - h_4)$$

and if for similarly designed stages the efficiency  $\eta_s$  is the same then

$$\eta_c = (W/m) / (h_{11} - h_1)$$

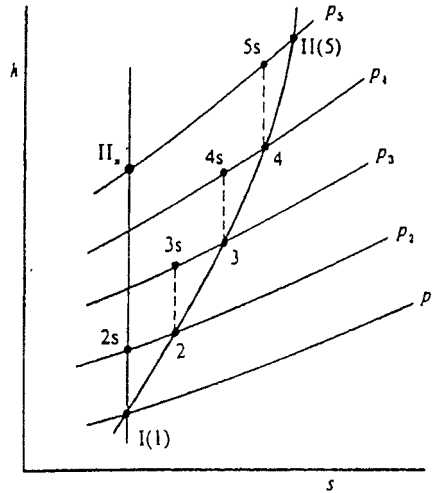


Fig. 3.20 Multi -stage compression

where the numerator consists of a number of isentropic enthalpy increases. But as the entropy increase through the compression, so the constant pressure lines diverge and

$$(h_{2s} - h_1) + (h_{3s} - h_2) + \dots > (h_{11s} - h_1)$$

and thus

$$\eta_s > \eta_c$$

That is, the overall single isentropic compression efficiency is less than the stage efficiency. The difference also increases with pressure ratio and with the number of stages.

To account for compression in stages, a small stage or polytropic efficiency is defined for an elemental compression process. This efficiency is considered to be constant throughout the whole compression. Assuming constant specific heat, then for the elemental compression in Fig 3.21

$$\eta_p = dT' / dT \tag{3.41}$$

For an isentropic process

$$T/p^{(\gamma-1)/\gamma} = \text{const} \tag{3.42}$$

Thus

$$dT' = \text{const} [p^{-(1-\gamma)} (\gamma - 1) / \gamma] dp$$

Substituting for  $dT'$  from Eq. (3.41) and for the constant in Eq. (3.42), then

$$\eta_p (dT/T) = [(\gamma - 1)/\gamma] (dp/p)$$

Integrating between the limits of the full compression from I to II,

$$\ln (T_{11}/T_1) = [(\gamma - 1)/\gamma \eta_p] \ln (p_{11}/p_1) \quad (3.43)$$

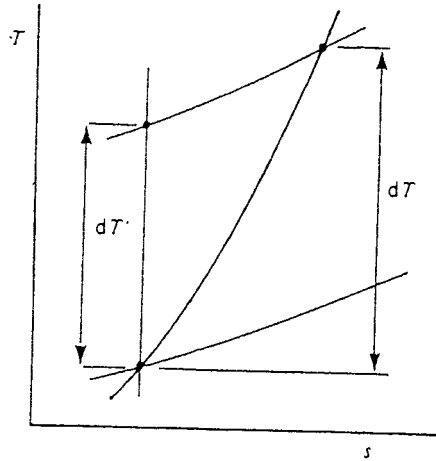


Fig. 3.21 Polytropic or small stage compression

and rearranging

$$p_{11}/p_1 = (T_{11}/T_1) \eta_p^{\gamma/(\gamma-1)} \quad (3.44)$$

A typical value for polytropic efficiency is 0.88 and in initial design calculations it is often assumed that

$$\eta_p = \eta_s.$$

If it is assumed that we have equal total temperature rises in each stage, and denoting the inlet conditions by 01 and outlet conditions at the last stage as 0II, then for N stages,

$$p_{011}/p_{01} = (T_{011}/T_{01}) \eta_p^{\gamma/(\gamma-1)} \quad (3.45)$$

$$\text{Also } T_{011}/T_{01} = (T_{01} + N\Delta T_0)/T_{01} \quad (3.46)$$

where  $\Delta T_0$  is the stage total temperature rise. It is also usual to assume that the polytropic and total-to-total stage isentropic efficiencies are equal at a value of about 0.88

While it is possible to make a very rapid calculation of pressure rise through the compressor by this method, the step-by-step calculation of conditions throughout the machine should still be made, particularly if blade forms change.

### Problems

Unless otherwise stated, the work done factor is unity and inlet stagnation conditions are 101.3 kPa and 288 K. For  $C_p = 1005 \text{ J/kg K}$ ;  $R = 287 \text{ J/kg K}$ ,  $\gamma = 1.4$

3.1 Using the notation given in the text show that in an axial flow compressor stage

$$h_2 - h_{2s} = (p_{01 \text{ rel}} - p_{02 \text{ ret}}) / \rho$$

3.2 An axial flow compressor stage with 50 per cent reaction has the following data;

|   |       |
|---|-------|
| Air inlet stagnation temperature                                      | 290 K |
| Relative flow angle at rotor outlet measured from the axial direction | 32°   |
| Flow coefficient  | 0.55  |
| Relative inlet Mach number onto the rotor                             | 0.75  |

If the stage is normal. what is the stagnation temperature rise in the first stage of the compressor.?

3.3 An axial flow compressor stage is to be designed for a stagnation temperature rise of 20 K. The work done factor is 0.92 and the blade velocities at the root mean radius and tip are 157.5, 210 and 262.5 m/s respectively. The axial velocity is constant from root to tip and is 157.5 m/s If the reaction ratio at the mean radius is 0.5, what are the inlet and outlet air and blade angles at the root, mean radius and tip for a free vortex design? Calculate also the reaction at the root and tip.

3.4 An alternative design proposal to that in exercise 3.3 is to have 50 percent reaction along the whole blade. What, then will the air and blade angle be?

3.5 The design of the first stage of an axial flow compressor calls for the following design data

|                                   |            |
|-----------------------------------|------------|
| Stage stagnation temperature rise | 22 K       |
| Mass flow of air                  | 25 kg/s    |
| Rotational speed                  | 150 rev/ s |
| Axial velocity through stage      | 157 m/s    |
| Work done factor                  | 0.95       |
| Mean blade speed                  | 200 m/s    |
| Reaction at the mean radius       | 50 percent |
| Rotor blade aspect ratio          | 3          |
| Inlet stagnation temperature      | 288 K      |
| Inlet stagnation pressure         | 101.3 kPa  |

Determine

- (a) the blade and air angles at the mean radius
- (b) the mean radius
- (c) the blade height
- (d) the pitch and chord and
- (e) the number of blades

3.6 Using the data of exercise 3.5, if a circular arc camber line for the blade is assumed, and also the data of Fig 3.13 determine.

- (a) the blade camber angle
- (b) the deviation
- (c) the blade stagger

- (d) the total drag coefficient of the blade
- (e) blade row efficiency and stage efficiency
- (f) stage static pressure ratio and
- (g) the stage total pressure ratio.

Assume zero incidence and a normal stage ( $C_1 = C_3$ )

3.7 An axial flow compressor has constant axial velocity through the compressor of 160m/s, a mean blade speed of 244m/s and delivers a pressure ratio of 5:1 Each stage is of 50 percent reaction and the relative outlet air angles are the same ( $30^\circ$ ) for each stage. If a polytropic efficiency of 88 per cent is assumed, determine the number of stages in the compressor.

3.8 An axial flow compressor delivers a total pressure ratio of 6. the total head pressure and temperature at entry being 0.408 M Pa and 300 K respectively and the overall isentropic efficiency being 82 percent. The degree of reaction is 50 percent and all stages contribute an equal amount of work. At a particular stage the blade speed at the mean height is 203 m/s and the axial velocity 171 m/s. If the absolute air angle entering the rotor at this stage is  $15^\circ$  and the work done factor is 0.92 determine

- (a) the rotor air inlet angle
- (b) the number of stages required
- (c) the static temperature of the air at entry to the rotor and
- (d) the rotor inlet relative Mach number

3.9 An axial flow compressor has 10 stages and the following data apply to each stage at the mean diameter.

|  |                    |
|--|--------------------|
| Blade speed                                    | 200 m/s            |
| Reaction                                       | 0.5                |
| Polytropic efficiency                          | 0.88               |
| Stage efficiency                               | 0.84               |
| Angle of absolute air velocity at rotor inlet  | $13^\circ$         |
| Angle of absolute air velocity at rotor outlet | $45^\circ$         |
| Work done factor                               | 0.86               |
| Inlet stagnation pressure                      | 99.3 k Pa          |
| Inlet stagnation temperature                   | $15^\circ\text{C}$ |

Determine the total pressure ratio of the first stage and the overall static pressure ratio.

3.10 An axial flow compressor under test in a laboratory exhibits a stage loading of 0.4 for a reaction ratio of 0.65 and flow coefficient 0.55. It is decided to reduce the mass flow by 7 percent while the blade speed is kept constant and it is assumed under this new condition that the relative flow exit angle for both the rotor and stator remain unchanged. What is the stage loading and reaction at the new condition? Assume the work done factor is 0.9

## REFERENCE

1. Burghardt, M.D., "Engineering Thermodynamics with Applications", 2nd Ed; Harper & Dow publication, N.Y., 1982
2. Eastop, T.D & Mc Conkey, A., "Applied Thermodynamics for Engineering Technologists". 3rd Ed., 3rd Impression Longman, Group Ltd. London, 1981.
3. Joel, Rayner, "Basic Engineering Thermodynamics in SI units", 3rd Ed., E.L.B.S., Longman Group Ltd. 1997.
4. Khurmi, R.S., "Applied Thermodynamics (in M.K.S. Units)", 1st Ed., s Chand & Co Ltd., New Delhi, 1997.
5. Kulshrestha, S.K., "A Textbook of Applied Thermodynamics, Steam and Thermal Engineering". 1st Ed., Vikas Publishing House Pvt Ltd., New Dehli, 1983.
6. Rogers, G.FC & Mayhew, Y.R., "Engineering Thermodynamics work and Heat Transfer (S.I units)". 2nd Ed., E.L.B.S & Longman Group Ltd., 1978
7. Cohen, H., "Gas Turbine Theory (SI units)", 2nd Ed., G.S.V Rogers, H.I.H Saravanamuttoo., 1972.